



Ke Wang^A, Ye Zhao^A, Lele Cong^A, Hongyan Sun^A, Hengxing Ba^B, Chunyi Li^B, Yimin Wang^{A,*} and Xianling Cong^{A,*}

For full list of author affiliations and declarations see end of paper

*Correspondence to:

Yimin Wang

China-Japan Union Hospital, Jilin University, No. 126, Xiantai Street, Erdao District, Changchun 130033, Jilin, P. R. China Email: yiminwang@jlu.edu.cn; Xianling Cong China-Japan Union Hospital, Jilin University, No. 126, Xiantai Street, Erdao District,

Changchun 130033, Jilin, P. R. China

Email: congxl@jlu.edu.cn

Handling Editor: Sathya Velmurugan

Received: 18 February 2022 Accepted: 25 April 2022 Published: 19 May 2022

Cite this:

Wang K et al. (2022) Animal Production Science doi:10.1071/AN22056

© 2022 The Author(s) (or their employer(s)). Published by CSIRO Publishing.

ABSTRACT

Context. Deer antlers offer a premium model for investigating the mechanisms underlying arguably the most rapid cartilage formation and remodelling system. Although the cartilage formation process in the antler has been relatively intensively studied, thus far, at a molecular level, the cartilage remodelling has essentially been untouched. Aims. To construct miRNA-mRNA regulatory networks for both the cartilage formation and remodel zones in the antler tip. Methods. The tissues from both the cartilage formation zone (FZ) and remodel zone (RZ) in rapid growing antlers of sika deer were sampled, profiles of both mRNA and miRNA from these samples were sequenced and analysed, miRNA-mRNA regulatory networks for these two zones were constructed, and their encoded/targeted differentially expressed genes (DEGs) were identified through bioinformatics analysis. Key results. In total, 3703 DEGs in the FZ over the RZ were identified, with 1615 being upregulated and 2088 downregulated. The upregulated DEGs in the FZ were found to be mainly enriched in cell proliferation and chondrogenesis/osteogenesis, whereas those in the RZ were enriched in the formation of chondroclasts and osteoclasts. In total, 308 unique mature miRNAs were detected including 110 significantly differentially expressed miRNAs. These miRNAs are predicted to target extracellular matrix proteins, growth factors and receptors, and transcriptional factors, all related to cartilage formation and remodelling. To verify the reliability of our datasets, we successfully tested the regulatory function of one of the top 10 hub miRNAs, miR-155, in vitro. Conclusions. The miRNA-mRNA regulatory networks for cartilage formation zone (FZ) in relation to cartilage remodel zone (RZ) were successfully constructed, and validated, which has laid the foundation for the identification of potent growth factors and novel regulation system in bone formation through endochondral ossification. Implications. We believe that our datasets are reliable for further mining potent growth factors and novel regulation systems for rapid cartilage formation, remodelling and bone fracture repair by using this unique model, the deer antler.

Keywords: antler, cartilage formation, miRNA, mRNA, regulatory networks, remodel zone, miR-155, FOXO3.

Introduction

A natural mammalian model system which possesses the fastest growth rate but does not become cancerous would provide a great opportunity to identify potent growth factors and unique regulatory systems. In this regard, the deer antler offers a premium example. Deer antlers are organs of bone, and above all can fully regenerate annually (Goss 1983; Li 2021; Li and Fennessy 2021). Each year in spring, totally calcified antlers (dead) are cast and regenerate from the pedicles (permanent bony protuberances); newly growing antlers grow at a phenomenal growth rate (up to 2 cm/day) in the late spring and early summer (Goss 1970), become fully calcified in autumn, which causes shedding of the velvet skin (unique pelage to antler), and hard antlers remain on top of the pedicles in winter,

till next spring (Li and Chu 2016). It is known that antler formation is achieved through modified endochondral ossification, and a growing antler consists of the following five zones: proliferation, maturation, hypertrophy, calcification and chondroclasia distoproximally (Banks Newbrey 1983). The antler growth centre (proliferation and cartilage maturation zones) occurs in its tip and consists of histologically distinguishable layers including the reserve mesenchyme, precartilage, and cartilage distoproximally. To enable studying the astonishing antler growth rate at the levels of cellular and molecular biology, a generally applicable and standardised sampling technique was developed to collect these tissue layers from the fresh and unprocessed antler tip (Li et al. 2002), which has greatly facilitated the progress of understanding the molecular mechanism underlying this fastest growth system.

The technique for sampling the tissue layers in the antler growth centre was first adopted for construction of the suppression subtractive cDNA library (Li et al. 2002), and, subsequently, used for the identification of differentially expressed genes (DEGs; potent factors) in the antler growth centre (Gyurján et al. 2007; Molnár et al. 2007; Yao et al. 2012). Recently, Hu et al. (2014, 2015) worked on microRNAs (miRNAs) and found that both miRNA-1 and miRNA-18A negatively regulate the most potent growth factor, insulin growth factor 1 (IGF1), thus far found in the antler growth centre. miRNA-mRNA regulatory networks were constructed in the antler growth centres (regulatory system; Yao et al. 2019; Jia et al. 2021). Overall, the antler growth centre, the proliferation and cartilage maturation zones [the cartilage formation zone (FZ)], has been intensively investigated at a molecular level, and some potent growth factors and novel regulatory networks have been identified. Nonetheless, the FZ constitutes only the first part of endochondral ossification taking place in antler formation; and the second part, the conversion from cartilage to bone tissue (cartilage remodel zone, RZ; including hypertrophy, calcification and chondroclasia), has essentially been untouched. However, understanding the process of the second part (RZ) and putting the findings from the FZ into the analysis for the RZ is critical if the mechanisms underlying the whole picture of this fastest-growing system are to be unveiled. The RZ is an integral part of the whole endochondral ossification process to sustain the most rapid growth FZ, which is taking place distally in the growing antler.

The aim of the present study was to build up the miRNA-mRNA regulatory networks for the FZ in relation to the RZ, so as to try to identify the potent factors and regulatory networks for chondrogenesis, and, thus, to understand this fastest growth system in a broader context than the currently available one.

Materials and methods

Tissue sampling

Tissue samples of both the FZ (Li and Suttie 2003), including reserve mesenchyme (RM), precartilage, transition zone and cartilage zone, and the RZ (Banks and Newbrey 1983) were collected from each of the three sticks of three-branch-antlers of three 3-year-old male sika deer. Briefly, the distal 7 cm of each growing antler tip was removed, and the FZ and the RZ tissues were surgically dissected respectively (Li et al. 2002), and cut into small pieces (1 mm³) for primary cell culture under an aseptic condition (Li et al. 1999).

RNA extraction, quantification and sequencing

Each tissue sample (FZ: n=3; and RZ: n=3) was rapidly ground into fine powder with Freezer/Mill 6770 (SPEX CertiPrep Ltd, USA) in liquid nitrogen. Total RNA was extracted and purified using Trizol reagent (Invitrogen, USA). RNA quality was measured using Agilent 2100 bioanalyser (Agilent Technologies Inc., USA), and the criteria were set as follows: \geq 60 ng/ μ L, 28 s/18 s \geq 0.8 and RIN \geq 7.5. Library preparation and sequencing of RNA-Seq and small RNA were performed using the BGISEQ-500 platform (Beijing Genomics Institute, Wuhan, China).

Bioinformatics analysis

Quality control and preprocessing of raw reads were performed using Fastp v0.11.8 (Chen et al. 2018). For the RNA-Seq data, the pair-end 100 bp clean read mapping and gene expression level quantification were performed using the workflows of HISAT2, StringTie, and DESeq2 (Pertea et al. 2016). Briefly, the reads were aligned against our published deer reference genome (Ba et al. 2020) by using HISAT v2.1.0 (Kim et al. 2015). Gene expression levels in each sample were estimated using StringTie v2.0 (Pertea et al. 2015). The Python script of prepDE.py was used to extract the read count information of each gene from the coverage values estimated by StringTie. On obtaining the results of prepDE.py, DEGs were detected using DESeq2 v1.18.1 (Love et al. 2014) on the basis of |log₂(fold change) ≥ 1 and adjusted *P*-value (Benjamini Hochberg) of ≤ 0.001 .

For the small RNA sequencing data, all unique single-end 50 bp clean reads were screened against Rfam v13.1 (http://rfam.xfam.org/) to remove non-miRNAs, such as rRNA, scRNA, snoRNA, snRNA and tRNA by performing BLASTn search with a 0.01 *E* value threshold. The resultant reads were used to identify known miRNAs by matching Bos taurus dataset (1064 precursors, 1025 mature miRNA) in miRBase v22.1 (http://www.mirbase.org/), using miRDeep2 with default parameters (Friedländer *et al.* 2012). Subsequently, our miRNA count expression profiling

was constructed. Differentially expressed miRNAs (DEmiRNAs) were also identified using DESeq2 v1.18.1 (Love *et al.* 2014) on the basis of the criteria setting at $|\log_2(\text{fold change})| \ge 1$ and adjustment *P*-value of ≤ 0.001 . To predict the target genes of our identified known miRNAs, both RNAhybrid v2.1.2 (Krüger and Rehmsmeier 2006) and miRanda v3.3a (Agarwal *et al.* 2015) were used. We also retrieved target genes of these miRNAs by using TargetScan v3.1 database (Lewis *et al.* 2005).

Online database, STRINGdb (https://string-db.org/), was used to construct the protein-protein interaction (PPI) network, with all interaction sources and minimum required interaction score being set at >0.4 for our target genes. The Cytoscape v3.6 (Shannon et al. 2003) was used to visualise protein-protein and miRNA target pairs network. Network statistics were performed through inhouse commands in the Cytoscape. Key hub nodes in the network were defined by their connective degrees with other nodes. Gene ontology (GO) and Kyoto Encyclopaedia of Genes and Genomes (KEGG) pathway analysis were performed by using gene set enrichment analysis (GSEA v.4.1.0) (Bean et al. 2020) on the basis of the Molecular Signatures Database v. 7.1. C5 with 1000 permutation number. We set the cut-off criteria as gene size of ≥ 15 and nominal P-value of < 0.01

Cell culture

Detailed procedures for antler cell isolation and culture were described in our previous study (Li et al. 1999). Briefly, collagenases I and II (1:1; 200 U/mL) were used to digest the RM and the RZ tissues respectively. Suspension of each cell digest was centrifuged at 224g for 5 min to remove digestive enzymes and the resultant cells were plated onto 75 cm² culture flasks and cultured in the culture medium, a low-glucose DMEM supplemented with 10% fetal bovine serum (FBS; Life Technology) and 100 U/mL penicillin and 100 mg/mL streptomycin (Sigma, San Francisco, CA, USA) at 37°C with saturated humidity and 5% CO2. Five days after culture, the non-adherent cells were removed through medium washing; thereafter, the culture medium was changed twice a week. The cells were passaged using trypsin (Sigma), and frozen in liquid nitrogen in cryovials containing freezing medium (DMEM:FBS:DMSO = 6:3:1). When required, cells were thawed and cultured in T75 flasks. The third passage of the antler cells was used in the subsequent study.

Cell proliferation assay using CCK8 method

The cultured cells (\sim 85% confluence) were trypsinised and gently pipetted up and down to make a single-cell suspension, and the number of cells were counted using trypan blue. After that, the cells were inoculated into a standard 96-well plate (10^3 cells/well). Once the cultured

cells reached 80% confluence, 10 μL of CCK8 detection reagent (APExBIO, USA) was added into each well, and the absorbance (450 nm) of each well was measured at 24 h, 36 h and 48 h respectively, and then 10 μL test solution from the kit was added into each well. The plate was wrapped using tin foil to avoid light and kept at room temperature for 2 h before measurement of the absorbance (OD) value; OD measurements were repeated three times for calculation of the average value.

Quantitative real-time RT-PCR (qRT-PCR)

For mRNA analysis, the specific primers were designed using Primer 5 and listed in Supplementary Table S1. Total RNA was first treated with DNase I, before reverse-transcription by superscript III double-stranded cDNA synthesis kit (Invitrogen Inc., Camarillo, CA, USA). GAPDH was used as a standard control according to our in-house selection standard. For miRNA analysis, stem-loop qRT-PCR method (Chen et al. 2005) was used to validate DEmiRNAs. All primers for miRNA are listed in Table S2. The reversetranscription reaction for miRNA was performed using the One Step PrimeScript RT reagent Kit (TaKaRa, Japan) according to the manufacturer's protocol, and U6 snRNA was used as an internal reference. A dissociation curve for each analysis (mRNA or miRNA) was obtained to ensure that only one product was amplified after the amplification phase. The qRT-PCR was performed using the SYBR Kit (Applied Biosystems, USA) according to the manufacturer's protocols (Applied Biosystems 7500 detection system). Relative expression level was calculated using the $2^{-\Delta\Delta CT}$ method. All reactions were performed in three replicates.

miRNA mimics transfection

The transfection experiment was divided into the following three groups by using RM cells: miR-155 Mimic group, mimic-NC group and control group. Twenty-four hours before transfection, cells were inoculated into 24-well plates (10⁵ cells/well), and the transfection was conducted when the cells grew to 70–90%. The miRNA mimics were diluted in Lipofectamine 2000 reagent (Life Technology, UK) and transfected into the RM cells of the miR-155 Mimic group, standing at room temperature for 10 min, and the cells were washed with serum-free DMEM medium twice. Thereafter, 3 mL of serum-free DMEM medium was added to the culture plates, and 20 min after standing at room temperature, the cells were transferred into a 37°C 5% CO₂ incubator for 48 h culture.

Ethical approval

The three sticks of growing deer velvet antlers were bought from a commercial deer farm, collected immediately after removal and brought into our cell-culture lab for further

processing. The removal procedure of velvet antlers was strictly in accordance with the guidelines of national velveting procedure (i.e. under full anaesthesia).

Results

Overall quality of RNA-sequencing dataset

High-throughput sequencing and the resultant mRNA and miRNA profiles for the samples from three biological replicates taken from each of the two zones (FZ and RZ) were analysed. For the mRNA analysis, 7.71–7.66 Gb of the low-quality reads and adapters in the six libraries (two zones × triplicates) were filtered, and the resultant 6.62–6.90 Gb clean reads were aligned onto our published deer genome (Ba *et al.* 2020), and the mapping rates were found to be within 92.61–93.96% (Table S3). For the miRNAs, about 27 726 209–29 951 845 raw reads were generated in the six miRNA libraries. After quality control, we obtained 26 393 663–27 558 556 clean miRNA reads (Table S4), and their lengths varied between 10 and 44 nucleotides in each

library, with majority of the reads having 21–23 nucleotides (Supplementary material Fig. S1). High-quality clean reads larger than 18 nucleotides were mapped onto our published deer genome, and the mapping rates were found to be within 90.58–95.7%. Further, by matching of these clean reads onto Rfam database, we detected and remved the reads that match rRNA, small nuclear RNA (snRNA), or small nucleolar RNA (snoRNA) (Table S5). Overall, these RNAs accounted for only 2.1% in the total RNA pool (3 495 061/163 408 776). The RNA expression patterns in the libraries of the FZ and the RZ showed significant difference based on pairwise Pearson correlation analysis (Fig. S2). Both of the high-quality RNA sequencing data (mRNA and miRNA) were used for further analysis.

DEGs of the FZ over the RZ

Our bioinformatic analyses were led to the identification of 3703 DEGs of the FZ over the RZ (Table S6). Of these DEGs, 1615 were upregulated and 2088 downregulated in the FZ (Fig. 1a, b). The results of GSEA showed that the upregulated DEGs in the FZ were enriched in GO

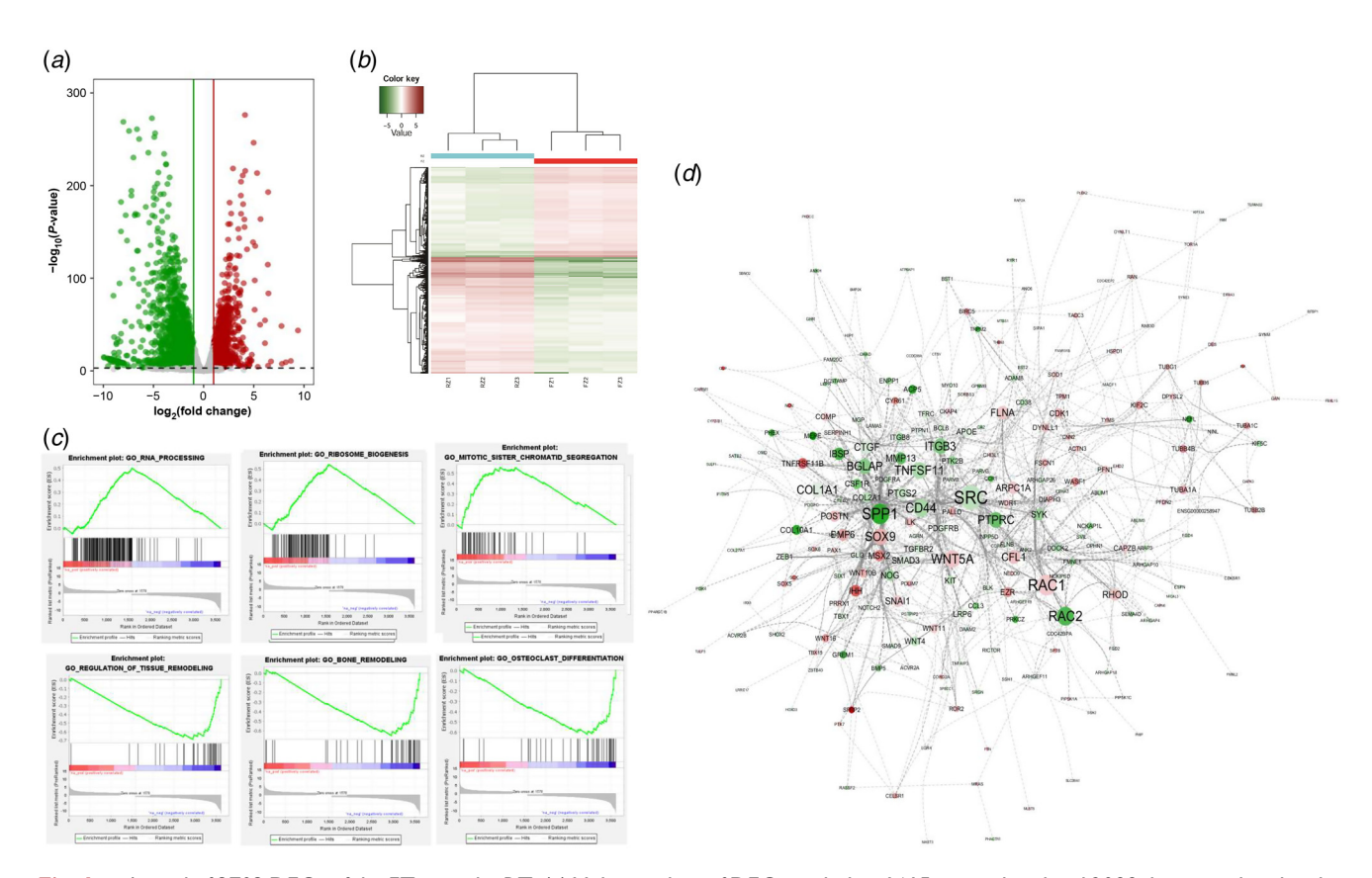


Fig. 1. A total of 3703 DEGs of the FZ over the RZ. (a) Volcano plots of DEGs, including 1615 upregulated and 2088 downregulated in the FZ. (b) Hierarchical clustering of these DEGs. (c) GSEA of these DEGs. (d) Interactive network consisted of 238 DEGs related to cartilage formation and remodelling, including 87 upregulated and 151 downregulated genes. Average number of neighbours was 10.1. Value of log₂(fold change) of genes is indicated by the grade of the colour. The size of the node indicates the degree of connectivity; the larger the node, the higher the degree of connectivity with others for a given gene. DEGs, differentially expressed genes; FZ, cartilage formation zone; RZ, cartilage remodel zone; GSEA, gene set enrichment analysis.

biological-process terms associated with chromosome segregation, RNA processing and ribosome biogenesis. The upregulated DEGs in the RZ were related to the regulation of tissue remodelling, bone remodelling and osteoclast differentiation (Fig. 1c, Table S7). The enriched KEGG pathways were also listed in Table S7, which were found to be consistent with the GO analysis results.

Protein-protein interaction network of the DEGs related to cartilage formation and remodelling

Next, 255 DEGs that were related to cartilage formation and remodelling were used to construct protein-protein interaction network by using STRINGdb, and further visualised by using Cytoscape. The network analysis results showed that the number of nodes was 238 (93.3%) and the average number of neighbours was 10.1, indicating that this interaction network derived from the DEGs is robust. The 87 upregulated DEGs in the FZ, including RAC1, WNT5A, SOX9, CFL1, FLNA, ARPC1A, BMP6, RHOD, SNAI1 and IHH, were found to be shared among most of the interactions and, thus, were termed as the FZ hub nodes. The 151 upregulated DEGs in the RZ group, including SRC, SPP1, RAC2, CD44, TNFSF11, COL1A1, PTPRC, ITGB3, BGLAP and CTGF, were termed as the RZ hub nodes (Fig. 1d). Relative expression levels of the randomly selected five hub genes (three upregulated and two downregulated) were validated using qRT-PCR, and the results showed high consistency with those of our RNA-seq data (Fig. 2a).

DEmiRNAs of the FZ over the RZ

In total, 308 unique mature miRNAs were identified from the 367 miRNA precursors (of the 153 566 803 reads) in the two

zones, namely, FZ and RZ (Table S8). Of these 308 mature miRNAs, 110 were found to be significantly DEmiRNAs in the FZ (Table S9). Of these 110 DEmiRNAs, 61 and 49 were significantly upregulated and downregulated respectively (Fig. 3*a*, *b*). The top 10 upregulated miRNAs were identified as miR-504, miR-2314, miR-370, miR-665, miR-543, miR-3957, miR-485, miR-495, miR-377 and miR-758. The top 10 downregulated miRNAs were identified as miR-2285cl, miR-429, miR-200a, miR-200b, miR-205, miR-31, miR-200c, miR-153, miR-326 and miR-486.

Integrated analysis of DEmiRNAs-DEGs target pairs

Of the 308 mature miRNAs, 193 were found to have 63 598 miRNA-target pairs containing 7523 unique genes (Fig. S3). Of these 63598 miRNA-target pairs, 2298 (3.6%) were opposite-direction regulatory pairs, including 36 upregulated miRNAs (upregulated in the FZ) that were predicted to negatively regulate 606 downregulated DEGs; and 40 downregulated miRNAs (upregulated in the RZ) that negatively regulate 461 upregulated DEGs. The network of the upregulated miRNAs and their targets was visualised by using Cytoscape. The top 10 hub miRNAs were identified via evaluating the connected degrees with their targets, including miR-125a, miR-125b, miR-92b, miR-204, miR-377, miR-7, miR-543, miR-33a, miR-155 and miR-381. The average target of these 10 miRNAs is 73.6. These miRNAs were found to target extracellular matrix proteins (e.g. COL1A2, ITGB3, COL2A1, VCAN and BGN), growth factors and receptors (e.g. WNT4, FGFR1, FGFRL1, TGFBR2, NOTCH2/3, SMAD6/7, INSR, PDGFRA, SRC and IGF2R) and transcription factors (e.g. FOXO3, FOSL2 and SIX1) (Fig. 3c). The top 10 downregulated hub miRNAs included miR-15a, miR-124a, miR-124b, miR-181b, miR-181a,

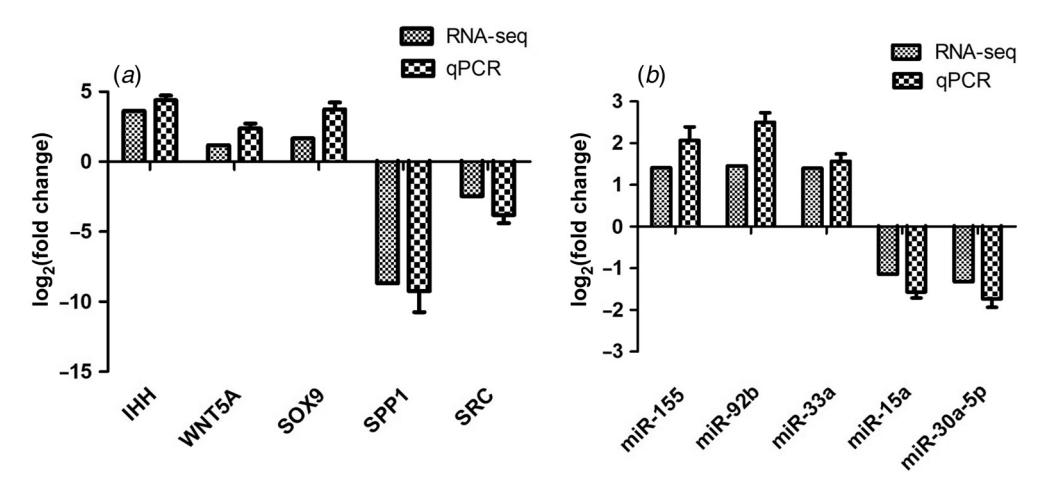


Fig. 2. Five randomly selected (a) mRNA and (b) miRNA from RNA-seq were verified using qRT-PCR analysis. Means of the normalised expression values (n = 3 pools) were calculated and are expressed as fold changes. The qRT-PCR data are expressed as means with s.d. bars. Note that results of both analyses were consistent. qRT-PCR, quantitative polymerase chain reaction.

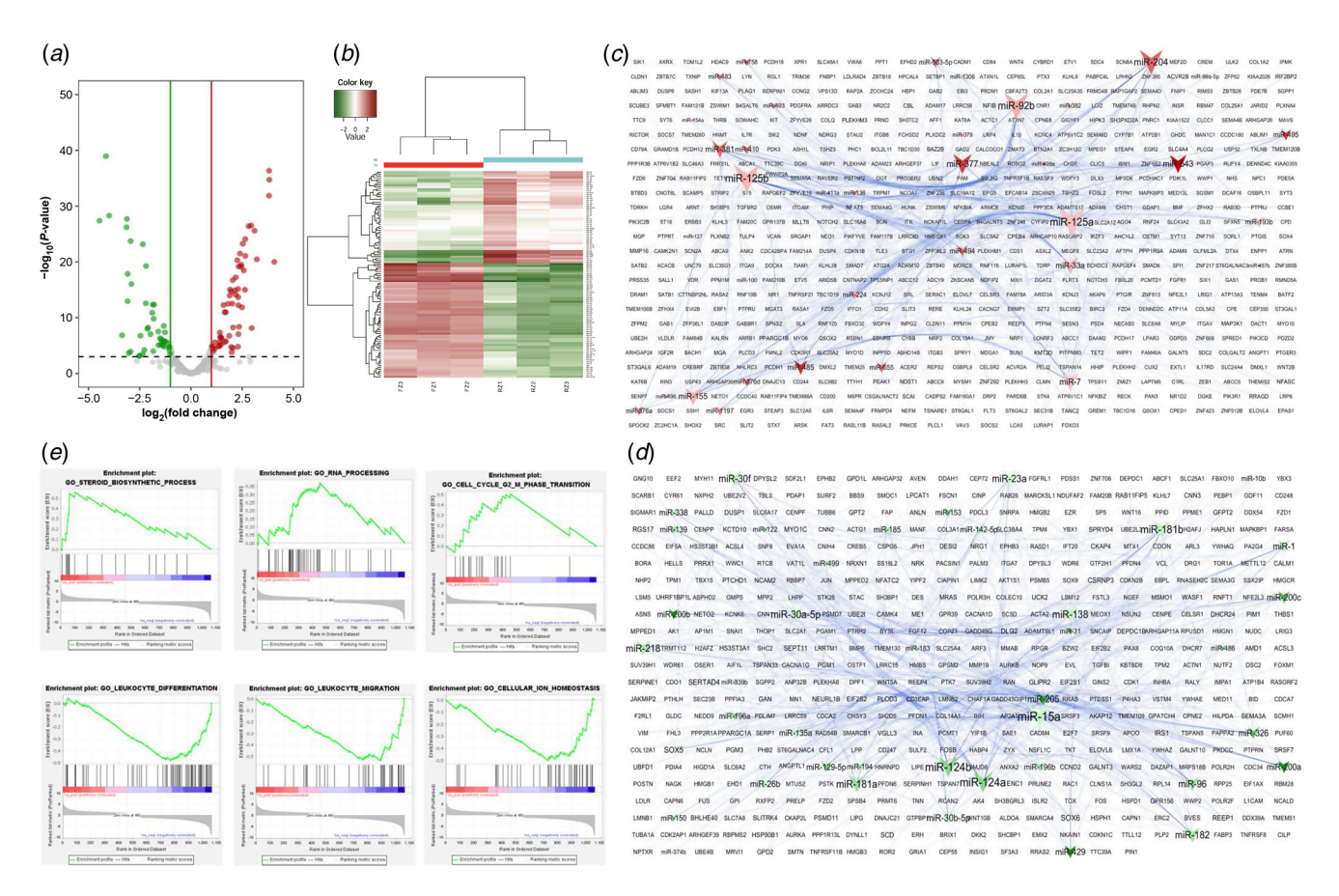


Fig. 3. Identification of DEmiRNAs in the FZ over the RZ. (a) Volcano plots of DEmiRNAs, including 61 upregulated and 49 downregulated in the FZ. (b) Hierarchical clustering of the identified DEmiRNAs. (c) Interaction network of 36 upregulated miRNAs and 606 downregulated target genes in the FZ. (d) Interaction network of 40 downregulated miRNAs and 461 upregulated target genes in the RZ. For the interaction network, value of log₂(fold change) of miRNAs is indicated by the grade of the colour. The size of the node indicates the degree of connectivity; the larger the node, the higher the degree of connectivity with others for a miRNAs. (e) GSEA of the target genes of these DEmiRNAs. DEmiRNAs, differentially expressed miRNAs.

miR-30a-5p, miR-138, miR-23a, miR-218 and miR-182. The average target of these 10 miRNAs is 48.4. These miRNAs were found to target extracellular matrix proteins (e.g. THBS1, VIM, MMP19, TNN and POSTN), growth factors and receptors (e.g. IHH, RXFP2, WNT16. WNT5A, BMP6, PTHLH and FGF12) and transcription factors (e.g. FOS, FOSB, JUN and SOX9) (Fig. 3d). These hub miRNAs were found to be key factors in regulating cartilage formation and remodelling respectively. Relative expression levels of the five randomly selected hub miRNAs (three upregulated and two downregulated) were validated using qRT-PCR, and high consistency with those of RNA-seq data was obtained (Fig. 2b).

Through analysis of 1067 differentially target genes (606 downregulated and 461 upregulated) by using GSEA, we found that the target genes in the FZ were mainly involved in steroid biosynthetic process, cell cycle and RNA processing. The target genes in the RZ were related to leukocyte differentiation, leukocyte migration and cellular ion homeostasis (Fig. 3e, Table S10). The results were

found to be consistent with those in DEGs between the two zones. However, no significant KEGG pathways were enriched.

Functional verification of miR-I55 and its target gene FOXO3

Relative expression level of the miR-155-mimic after transfection to the RM (the outmost layer of the FZ) cells was measured using qRT–PCR. The results showed that compared with the negative and blank controls, relative expression level of the miR-155-mimic in the transfected group increased significantly (P < 0.001; Fig. 4a). The relative expression levels of the FOXO3, the target gene of miR-155, in the RM cells were measured using qRT–PCR after the miR-155-mimic transfection. The results showed that compared with the blank and negative controls, the relative expression levels of the FOXO3 were significantly decreased (P < 0.001; Fig. 4b). Compared with the blank and negative controls, proliferation rate of the RM cells

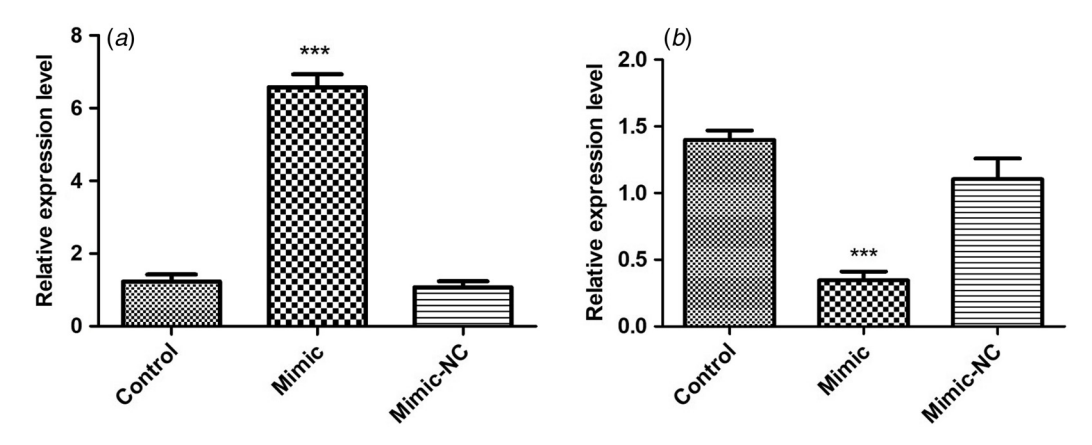


Fig. 4. Effects of transfection with miR-155 mimics on expression of the target gene FOXO3 in differently treated groups. (a) Expression levels of miR-155. (b) Expression levels of FOXO3. FOXO3, Forkhead Box Protein O3. ***P < 0.001.

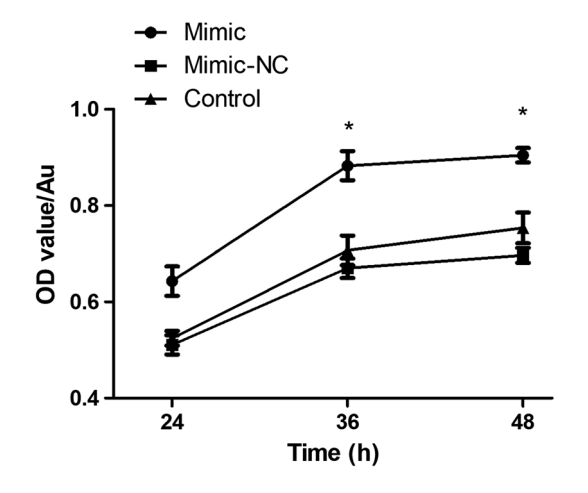


Fig. 5. Effects of miR-155 mimics transfection on the RM cell proliferation at the time points of 24, 36 and 48 h. *P < 0.05.

measured using CCK8 at the time points of 24, 36 and 48 h were significantly increased (P < 0.05; Fig. 5). All these results demonstrated that a decrease in the expression level of FOXO3 would result in an increase in the proliferation rate of the RM cells, and an increase in the expression level of the miR-155 would downregulate expression of its target gene FOXO3. Therefore, a high relative expression level of the miR-155 stimulates proliferation of the RM cells, which is the main driver for the most rapid antler growth.

Discussion

Deer antlers are arguably the fastest-growing organs of bone, and thus offer a unique opportunity to identify potent factors that drive antler growth to such a speed (2 cm/day; Goss 1970) and to unveil the novel regulation systems for cartilage/bone formation and remodelling. To the best of

our knowledge, this is the first report of construction of the miRNA-mRNA regulatory networks for the antler growth centre (cartilage formation zone, FZ) in relation to cartilage remodel zone (RZ). In the present study, the miRNA-mRNA regulatory networks of the two zones were constructed, compared and validated; and a number of hub DEGs and DEmiRNAs for rapid growth and cartilage remodelling were identified from the networks. Overall, our study has laid the foundation for further identification and evaluation of the potent factors and novel regulation systems for rapid cartilage formation and remodelling.

It is known that interactions between miRNAs and proteincoding genes play an indispensable role in tissue growth, differentiation and development (Lu and Clark 2012). In the present study, 3703 DEGs in the FZ over the RZ were identified, with 1615 being upregulated and 2088 downregulated. On the basis of the constructed proteinprotein interaction network in the present study, 89 hub genes (the most shared genes in the network) were identified in the FZ, and 166 hub genes were identified in the RZ. In total, 308 unique mature miRNAs were detected, including 110 significantly DEmiRNAs (61 upregulated in the FZ and 49 upregulated in the RZ). These miRNAs are predicted to target extracellular matrix proteins, growth factors and receptors, and transcriptional factors, which are likely to be key factors in regulating cartilage formation and remodelling respectively. Of these 308 mature miRNAs, 193 were found to have miRNA-target pairs, including 36 miRNAs upregulated in the FZ that are predicted to negatively regulate 606 downregulated DEGs; and 40 miRNAs upregulated in the RZ that are predicted to negatively regulate 461 upregulated DEGs. Overall, the upregulated DEGs identified through the above approaches in the FZ are found to be mainly enriched in cell proliferation and chondrogenesis/osteogenesis, whereas the upregulated DEGs in the RZ were enriched in the formation of chondroclasts and osteoclasts, the main players for chondroclasia and

osteoclasia. Consequently, our results are consistent with the biological functions of the sampled antler tissue types.

Of the top 10 downregulated hub miRNAs in the present study, miR-182 negatively targets parathyroid hormone-like hormone (PTHLH). This is the first time for PTHLH to be identified involving in the chondrogenesis of the antler growth centre, and this molecule is known to play important roles in many biological processes (Martin 2016), including regulation of endochondral bone formation, increase of endochondral ossification and promotion of recruitment and survival of osteoblasts. PTHLH together with its receptor inhibits hypertrophic differentiation of pre-hypertrophic chondrocytes (Vortkamp et al. 1996). It has been reported that miR-182-5p is a novel regulator of chondrogenesis (Bai et al. 2019), and its knock-down increases glycosaminoglycan (GAG) production, SOX9 and type II collagen expression as well as cell proliferation. Type II collagen is the main component of extracellular matrix in cartilage, and SOX9 plays a key role in chondrocyte differentiation and skeletal development, and is absolutely required for pre-cartilaginous condensation, the first step in chondrogenesis during which skeletal progenitors differentiate into chondroblasts (Matsushita et al. 2013). Overall, miR-182-5p regulates chondrogenesis via its target gene PTHLH (Bai et al. 2019). In the present study, through network analysis, we found that both PTHLH and SOX9 were negatively regulated by miR-182, and due to the fact that miR-182 was downregulated in the FZ, chondrogenesis must be enhanced in the zone.

Of the top 10 upregulated hub miRNAs in the present study, miR-155 negatively targets Forkhead Box Protein O3 (FOXO3), a molecule has never been reported in the antler development thus far. FOXO3 is a transcriptional factor that regulates different cellular processes, including cell-cycle arrest, differentiation, resistance to oxidative stress, and apoptosis (Salih and Brunet 2008), and regulation of the self-renewal of adult hematopoietic stem cells (HSC) (Miyamoto et al. 2017; Tothova et al. 2017). FOXO3 maintains the NSC pool by inducing a program that promotes quiescence, prevents premature differentiation, and controls oxygen metabolism (Renault et al. 2009). FOXO3 is required for the self-renewal of muscle SCs during muscle regeneration (Gopinath et al. 2014). Besides, FOXO3 also acts as a key regulator for chondrogenic commitment of skeletal progenitor cells where lipid availability is limited and promotion of SOX9 expression through directly binding to its receptor (van Gastel et al. 2020). It is also reported that the role in the maintenance of stem cell pool played by FOXO3 is realised through direct binding to the FOXO-responsive elements in the promoters of the Notch3 genes (Gopinath et al. 2014).

In the present study, through network analysis, we found that miR-155 negatively targets transcriptional factors FOXO3 and SOX9, and receptor NOTCH2/3. Therefore, it is likely that downregulated FOXO3 and NOTCH3 would

promote proliferation of RM cells, but impair chondrogenic commitment of pre-cartilaginous cells. To confirm whether FOXO3 plays a similar role in chondrogenesis as in the other systems described above and to verify the reliability of our generated datasets, we conducted an in vitro validation study. The results convincingly demonstrated that downregulation of miR-155 significantly reduced FOXO3 expression and, subsequently, impaired proliferation of RM cells. Therefore, we believe that the datasets used for the construction of miRNA-mRNA regulatory networks for antler growth centre (FZ) in relation to cartilage remodel zone (RZ) are reliable for further mining potent factors and novel regulation systems for rapid cartilage formation and remodelling by using this unique model. Each year, over 1 million people in the USA alone suffer the illness of bone fracture (Li et al. 2021). While bone fracture healing has to be achieved through endochondral ossification (Ma et al. 2022), and the outcome is often associated with limited mobility due to slow and impaired healing process. To enhance the process, potent factors for cartilage formation and remodelling are greatly needed. In this regard, antler model offers a unique opportunity for sourcing them.

Supplementary material

Supplementary material is available online.

References

Agarwal V, Bell GW, Nam J-W, Bartel DP (2015) Predicting effective microRNA target sites in mammalian mRNAs. *eLife* **4**, e05005. doi:10.7554/eLife.05005

Ba H, Cai Z, Gao H, Qin T, Liu W, Xie L, Zhang Y, Jing B, Wang D, Li C (2020) Chromosome-level genome assembly of Tarim red deer, Cervus elaphus yarkandensis. Scientific Data 7, 187. doi:10.1038/ s41597-020-0537-0

Bai M, Yin H, Zhao J, Li Y, Wu Y (2019) miR-182-5p overexpression inhibits chondrogenesis by down-regulating PTHLH. Cell Biology International 43, 222–232. doi:10.1002/cbin.11047

Banks WJ, Newbrey JW (1983) Light microscopic studies of the ossification process in developing antlers. In 'Antler development in Cervidae'. (Ed. RD Brown) pp. 231–260. (Caesar Kleberg Wildlife Research Institute)

Bean DM, Al-Chalabi A, Dobson RJB, Iacoangeli A (2020) A knowledge-based machine learning approach to gene prioritisation in amyotrophic lateral sclerosis. *Genes* 11, 668. doi:10.3390/genes11060668

Chen C, Ridzon DA, Broomer AJ, Zhou Z, Lee DH, Nguyen JT, Barbisin M, Xu NL, Mahuvakar VR, Andersen MR, Lao KQ, Livak KJ, Guegler KJ (2005) Real-time quantification of microRNAs by stem-loop RT-PCR. *Nucleic Acids Research* 33, e179. doi:10.1093/nar/gni178

Chen S, Zhou Y, Chen Y, Gu J (2018) fastp: an ultra-fast all-in-one FASTQ preprocessor. *Bioinformatics* **34**, i884–i890. doi:10.1093/bioinformatics/btv560

Friedländer MR, Mackowiak SD, Li N, Chen W, Rajewsky N (2012) miRDeep2 accurately identifies known and hundreds of novel microRNA genes in seven animal clades. *Nucleic Acids Research* **40**, 37–52. doi:10.1093/nar/gkr688

Gopinath SD, Webb AE, Brunet A, Rando TA (2014) FOXO3 promotes quiescence in adult muscle stem cells during the process

of self-renewal. Stem Cell Reports 2, 414–426. doi:10.1016/j.stemcr. 2014.02.002

- Goss RJ (1970) SECTION III. BASIC SCIENCES AND PATHOLOGY 24. Problems of antlerogesis. *Clinical Orthopaedics and Related Research* **69**, 227–238. doi:10.1097/00003086-197003000-00025
- Goss RJ (1983) 'Deer antlers: regeneration, function, and evolution.' (Academic Press: New York, NY, USA)
- Gyurján I Jr, Molnár A, Borsy A, Stéger V, Hackler L Jr, Zomborszky Z, Papp P, Duda E, Deák F, Lakatos P, Puskás LG, Orosz L (2007) Gene expression dynamics in deer antler: mesenchymal differentiation toward chondrogenesis. *Molecular Genetics and Genomics* 277, 221–235. doi:10.1007/s00438-006-0190-0
- Hu W, Li T, Wu L, Li M, Meng X (2014) Identification of microRNA-18a as a novel regulator of the insulin-like growth factor-1 in the proliferation and regeneration of deer antler. *Biotechnology Letters* **36**, 703–710. doi:10.1007/s10529-013-1428-7
- Hu W, Li M, Hu R, Li T, Meng X (2015) microRNA-18b modulates insulinlike growth factor-1 expression in deer antler cell proliferation by directly targeting its 3' untranslated region. DNA and Cell Biology 34, 282–289. doi:10.1089/dna.2014.2421
- Jia B, Zhang L, Zhang Y, Ge C, Yang F, Du R, Ba H (2021) Integrated analysis of miRNA and mRNA transcriptomic reveals antler growth regulatory network. *Molecular Genetics and Genomics* 296, 689–703. doi:10.1007/s00438-021-01776-z
- Kim D, Langmead B, Salzberg SL (2015) HISAT: a fast spliced aligner with low memory requirements. *Nature Methods* 12, 357–360. doi:10.1038/nmeth.3317
- Krüger J, Rehmsmeier M (2006) RNAhybrid: microRNA target prediction easy, fast and flexible. *Nucleic Acids Research* **34**, W451–W454. doi:10.1093/nar/gkl243
- Lewis BP, Burge CB, Bartel DP (2005) Conserved seed pairing, often flanked by adenosines, indicates that thousands of human genes are microRNA targets. *Cell* **120**, 15–20. doi:10.1016/j.cell.2004.12.035
- Li C (2021) Residual antler periosteum holds the potential to partially regenerate lost antler tissue. *Journal of Experimental Zoology Part A: Ecological and Integrative Physiology* **335**, 386–395. doi:10.1002/jez.2451
- Li C, Chu W (2016) The regenerating antler blastema: the derivative of stem cells resident in a pedicle stump. *Frontiers in Biosciences* (*Landmark Ed*) **21**, 455–467. doi:10.2741/4401
- Li C, Fennessy P (2021) The periosteum: a simple tissue with many faces, with special reference to the antler-lineage periostea. *Biology Direct* **16**, 17. doi:10.1186/s13062-021-00310-w
- Li C, Suttie JM (2003) Tissue collection methods for antler research. European Journal of Morphology 41, 23–30. doi:10.1076/ejom.41.1. 23.28106
- Li C, Littlejohn RP, Suttie JM (1999) Effects of insulin-like growth factor 1 and testosterone on the proliferation of antlerogenic cells *in vitro*. *Journal of Experimental Zoology* **284**, 82–90. doi:10.1002/(SICI) 1097-010X(19990615)284:1#x003C;82::AID-JEZ11#x003E;3.0. CO;2-K
- Li C, Clark DE, Lord EA, Stanton J-AL, Suttie JM (2002) Sampling technique to discriminate the different tissue layers of growing antler tips for gene discovery. *The Anatomical Record* 268, 125–130. doi:10.1002/ar.10120
- Li C, Mills Z, Zheng Z (2021) Novel cell sources for bone regeneration. *MedComm* 2, 145–174. doi:10.1002/mco2.51
- Love MI, Huber W, Anders S (2014) Moderated estimation of fold change and dispersion for RNA-seq data with DESeq2. *Genome Biology* 15, 550. doi:10.1186/s13059-014-0550-8
- Lu J, Clark AG (2012) Impact of microRNA regulation on variation in human gene expression. *Genome Research* 22, 1243–1254. doi:10.1101/gr.132514.111
- Ma C, Liu H, Wei Y, Li H, Miao D, Ren Y (2022) Exogenous PTH 1-34 attenuates impaired fracture healing in endogenous PTH deficiency mice *via* activating indian hedgehog signaling pathway and

- accelerating endochondral ossification. Frontiers in Cell and Developmental Biology 9, 750878. doi:10.3389/fcell.2021.750878
- Martin TJ (2016) Parathyroid hormone-related protein, its regulation of cartilage and bone development, and role in treating bone diseases. *Physiological Reviews* **96**, 831–871. doi:10.1152/physrev.00031.2015
- Matsushita M, Kitoh H, Kaneko H, Mishima K, Kadono I, Ishiguro N, Nishimura G (2013) A novel SOX9 H169Q mutation in a family with overlapping phenotype of mild campomelic dysplasia and small patella syndrome. *American Journal of Medical Genetics Part A* **161A**, 2528–2534. doi:10.1002/ajmg.a.36134
- Miyamoto T, Fukuda T, Nakashima M, Henzan T, Kusakabe S, Kobayashi N, Sugita J, Mori T, Kurokawa M, Mori S-i (2017) Donor lymphocyte infusion for relapsed hematological malignancies after unrelated allogeneic bone marrow transplantation facilitated by the Japan marrow donor program. *Biology of Blood and Marrow Transplantation* 23, 938–944. doi:10.1016/j.bbmt.2017.02.012
- Molnár A, Gyurján I, Korpos E, Borsy A, Stéger V, Buzás Z, Kiss I, Zomborszky Z, Papp P, Deák F, Orosz L (2007) Identification of differentially expressed genes in the developing antler of red deer Cervus elaphus. *Molecular Genetics and Genomics* **277**, 237–248. doi:10.1007/s00438-006-0193-x
- Pertea M, Pertea GM, Antonescu CM, Chang T-C, Mendell JT, Salzberg SL (2015) StringTie enables improved reconstruction of a transcriptome from RNA-seq reads. *Nature Biotechnology* **33**, 290–295. doi:10.1038/nbt.3122
- Pertea M, Kim D, Pertea GM, Leek JT, Salzberg SL (2016) Transcript-level expression analysis of RNA-seq experiments with HISAT, StringTie and Ballgown. *Nature Protocols* 11, 1650–1667. doi:10.1038/nprot. 2016.095
- Renault VM, Rafalski VA, Morgan AA, Salih DAM, Brett JO, Webb AE, Villeda SA, Thekkat PU, Guillerey C, Denko NC, Palmer TD, Butte AJ, Brunet A (2009) FoxO3 regulates neural stem cell homeostasis. *Cell Stem Cell* 5, 527–539. doi:10.1016/j.stem.2009.09.014
- Salih DAM, Brunet A (2008) FoxO transcription factors in the maintenance of cellular homeostasis during aging. *Current Opinion in Cell Biology* **20**, 126–136. doi:10.1016/j.ceb.2008.02.005
- Shannon P, Markiel A, Ozier O, Baliga NS, Wang JT, Ramage D, Amin N, Schwikowski B, Ideker T (2003) Cytoscape: a software environment for integrated models of biomolecular interaction networks. *Genome Research* **13**, 2498–2504. doi:10.1101/gr.1239303
- Tothova Z, Krill-Burger JM, Popova KD, Landers CC, Sievers QL, Yudovich D, Belizaire R, Aster JC, Morgan EA, Tsherniak A, Ebert BL (2017) Multiplex CRISPR/Cas9-based genome editing in human hematopoietic stem cells models clonal hematopoiesis and myeloid neoplasia. *Cell Stem Cell* 21, 547–555.e8. doi:10.1016/j.stem.2017.07.015
- van Gastel N, Stegen S, Eelen G, Schoors S, Carlier A, Daniëls VW, Baryawno N, Przybylski D, Depypere M, Stiers P-J, Lambrechts D, Van Looveren R, Torrekens S, Sharda A, Agostinis P, Lambrechts D, Maes F, Swinnen JV, Geris L, Van Oosterwyck H, Thienpont B, Carmeliet P, Scadden DT, Carmeliet G (2020) Lipid availability determines fate of skeletal progenitor cells *via* SOX9. *Nature* 579, 111–117. doi:10.1038/s41586-020-2050-1
- Vortkamp A, Lee K, Lanske B, Segre GV, Kronenberg HM, Tabin CJ (1996) Regulation of rate of cartilage differentiation by Indian hedgehog and PTH-related protein. *Science* **273**, 613–622. doi:10.1126/science.273. 5275.613
- Yao B, Zhao Y, Wang Q, Zhang M, Liu M, Liu H, Li J (2012) De novo characterization of the antler tip of Chinese Sika deer transcriptome and analysis of gene expression related to rapid growth. Molecular and Cellular Biochemistry 364, 93–100. doi:10.1007/s11010-011-1209-3
- Yao B, Zhang M, Liu M, Lu B, Leng X, Hu Y, Zhao D, Zhao Y (2019) Identification of the miRNA-mRNA regulatory network of antler growth centers. *Journal of Biosciences* 44, 11. doi:10.1007/s12038-018-9835-5

Data availability. The datasets generated during the current study are available in SRA under accession number of PRJNA784148.

Conflicts of interest. The authors declare that they have no competing interests.

Declaration of funding. This work was supported by National Natural Science Foundation of China (U20A20403 and 31901058); Science and Technology Foundation of Jilin Province of China (20210402030GH, 20210204150YY and 2021C017).

Author affiliations

AChina-Japan Union Hospital, Jilin University, No. 126, Xiantai Street, Erdao District, Changchun 130033, Jilin, P. R. China.

^BInstitute of Antler Science and Product Technology, Changchun Sci-Tech University, Changchun 130600, Jilin, P. R. China.